Green Synthesis and Characterization of Bismuth Ferrite Nanoparticles by using Neuracanthus trinervius leaf extract

Yogini S. Pagare[1,2], Nilesh N. Mharsale[2], Dnyaneshwar S. Khandbahale[1]

[1]Department of Botany, M.V.P. Samaj's K.R.T. Arts, B.H. Commerce and A.M. Science (KTHM) College, Nashik, Maharashtra, India, 422002

[2]Department of Physics, MVP Samaj's Arts, Commerce & Science College, Tryambakeshwar, Maharashtra, India, 422212

Abstract: In the field of green synthesis, production of nanoparticles by using plant extracts is very attractive approach. Our study aimed to achieve a green synthesis of bismuth ferrite nanoparticles by using ethanolic extract of *Neuracanthus trinervius* leaves. The physical properties of synthesized bismuth ferrite nanoparticles were characterized using XRD, UV-Vis spectrophotometer, FTIR spectrometer, SEM and EDS. The crystallite size is approximately 16.52 nm by Scherrer equation.

Key Words: Green synthesis, Extract, Bismuth ferrite, *Neuracanthus trinervius*.

I. INTRODUCTION

Nanoparticles are tiny particles that are 1–100 nm in diameter, which is one billionth of a meter. The most common types of nanoparticles are metals, metal oxides, carbon based, and quantum dots. Owing to their unique sizes and properties, nanoparticles have attracted significant attention in various fields including medicine, electronics, energy, and environmental science [1, 2]. There are many methods for synthesizing nanoparticles, including physical, chemical, and biological processes [3]. Green synthesis, is the eco-friendly and sustainable method of production of nanoparticles without the use of hazardous chemicals or toxic solvents, has gained attention in recent years within biological processes. Natural sources, such as plants and microorganisms, are popular green synthesis approaches [4]. Therefore, green/biological synthesis of nanoparticles is possible alternative to chemical and physical methods.

In recent years, the development of environmentally benign and sustainable methods for nanoparticle synthesis has garnered significant attention. Green synthesis, which utilizes plant-based extracts as reducing and stabilizing agents, offers a promising alternative to conventional chemical and physical methods that often involve hazardous substances and high energy consumption. Bismuth ferrite nanoparticle is a good candidate of metal oxide for various applications, in preparation of nanostructures [5], photocatalyst [6], Solid oxide fuel cell [8], gas sensor [9], catalyst for oxidation of hydrocarbons [10], water purification [11], photovoltaic [12], biomedical [13, 14] and antibacterial effect [15].

In this study, we report a green synthesis approach for the fabrication of bismuth ferrite nanoparticles using the aqueous leaf extract of Neuracanthus trinervius, a medicinal plant known for its phytochemical richness. This work not only contributes to the growing field of green nanotechnology but also highlights the potential of Neuracanthus trinervius as a viable biological resource for nanoparticle synthesis.

II. MATERIALS AND EXPERIMENTAL METHODS

2.1. Materials:

All chemicals were analytical grade. Ethanol was used for making plant extract. Bismuth(III) nitrate pentahydrate (Bi(NO3)3 · 5H2O) and Ferric nitrate (Fe(NO3)3·9H2O) are used as precursor. The fresh

leaves of *Neuracanthus trinervius* Wight were used to make ethanolic extract as reducing agent for the green synthesis of bismuth ferrite nanoparticles.

2.2. Green synthesis of bismuth ferrite nanoparticles:
Neuracanthus trinervius Wight, is the member of the family Acanthaceae [16, 17]. Firstly, the *N. trinervius* plants are collected, and their leaves were washed by tap water and then distilled water to remove soil & dust particles. Then leaves are shade dried and grind into powder form.

By using this powder, ethanolic extract is prepared by Soxhlet method. For the green synthesis of bismuth ferrite nanoparticles, the amount of 9.70 gm of $BiFeO_3$ is mixed with 10ml of plant extract and stirred continuously for one hour on magnetic stirrer. Gel form of solution was obtained. This obtained form was heated at 500^0C in rotatory evaporator for 2 hours to obtained powdered form and to ensure the removal of impurities [Fig. 1].

Fig.1: Flowchart for the producing bismuth nanoparticles using a green synthesis approach
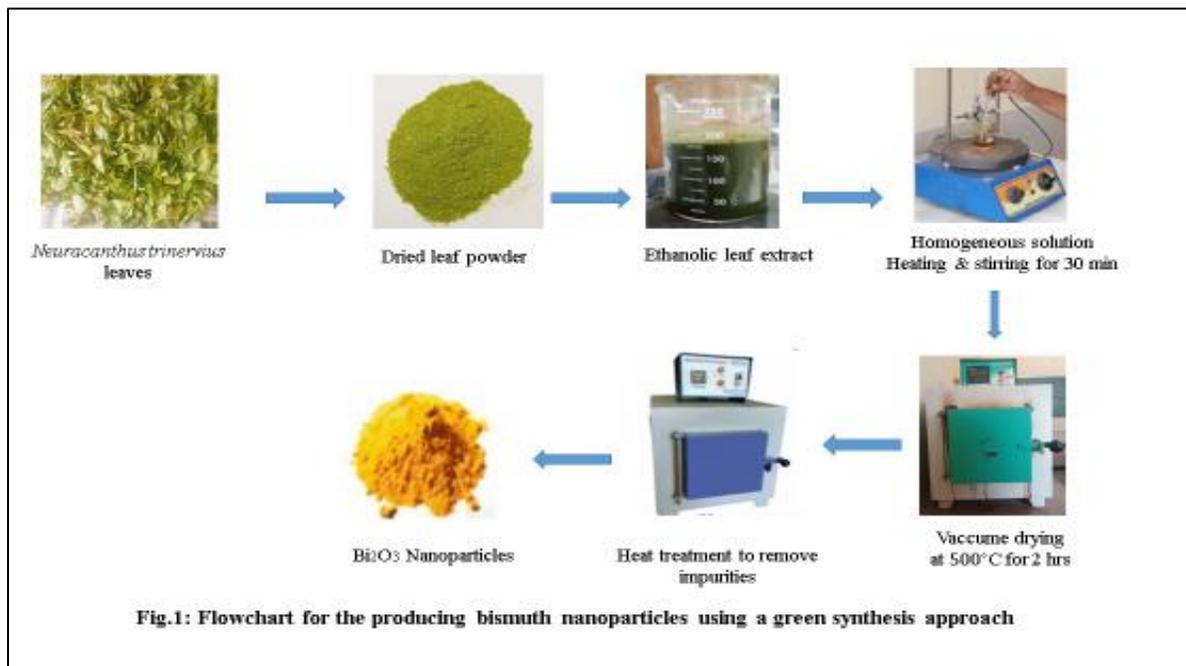
III.   RESULT AND DISCUSSION

The characterisation of synthesised nanoparticles was done in the department of physics, SPPU. The optimum time of synthesized nanoparticles was analysed by UV-Visible spectrophotometer for solution sample. X-Ray Diffraction (XRD) method was performed for evaluation of crystalline structure of bismuth ferrite oxide nanoparticles. Scanning electron microscope (SEM) was employed to observe the morphology and size of nanoparticles.

3.1. XRD:
The X-Ray diffraction technique was used to determine the crystalline structure of bismuth ferrite nanoparticles. The peaks of prepared sample match with characteristics peaks of JCPDS card #00-210-2910 for $BiFeO_3$ which shows the formation of the pure $BiFeO_3$ nanoparticles at 500^0C. Fig.2 shows the XRD pattern of prepared samples and the major diffraction peaks at specific 2θ values, such as those corresponding to (10-2), (104), (202), (216), (300), and higher-order planes.
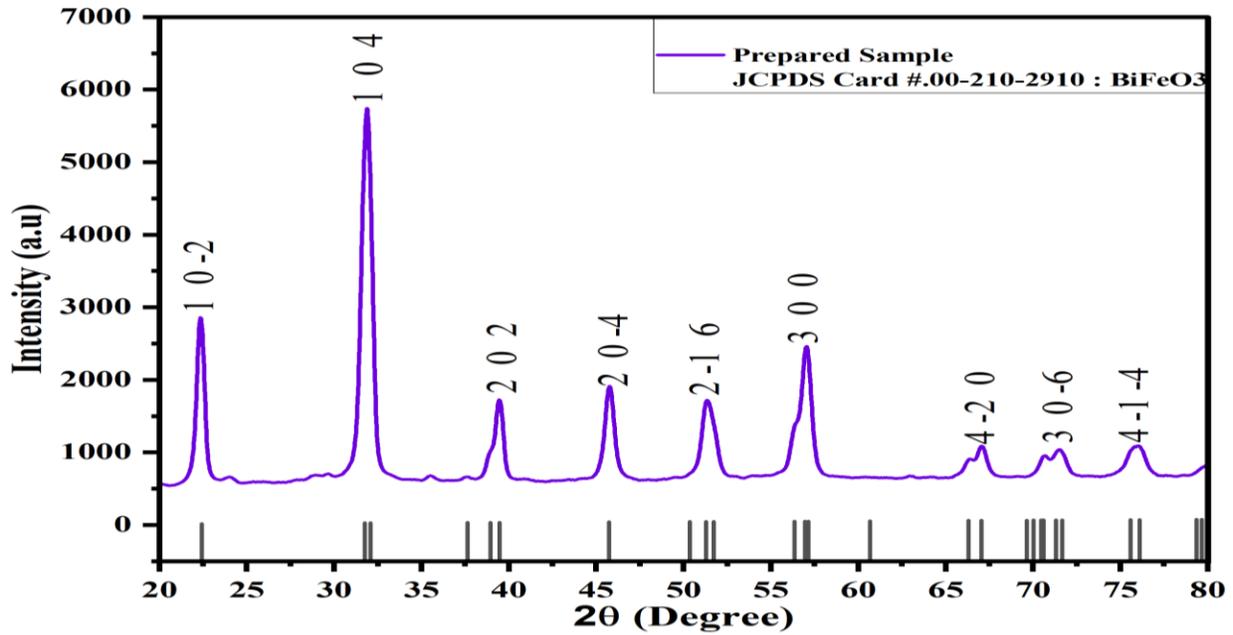
Fig.2. X-ray Diffraction Pattern at 500^0C

The sharp and distinct peaks in the pattern indicate a good degree of the crystallinity in the synthesized $BiFeO_3$ sample. The alignment with the standard JCPDS pattern suggests the sample predominantly belongs to the rhombohedral perovskite structure of $BiFeO_3$. The crystallite size can be estimated using the Scherrer equation [18]:

$$D = \frac{k\lambda}{\beta \cos \theta}$$

Where D = crystallite size, k = shape factor (~0.9 for spherical crystals), λ = wavelength of the X-ray (typically Cu Kα, ~1.5406 Å), β= full width at half maximum (FWHM) in radians and θ= Bragg angle. The crystallite size D is approximately 16.52 nm.

3.2. Scanning Electron Morphology (SEM):

For the analysis of the surface morphology, scanning electron microscope is used. The nanoparticles have been measured and annotated with sizes ranging from approximately 18.93 nm to 46.04 nm.
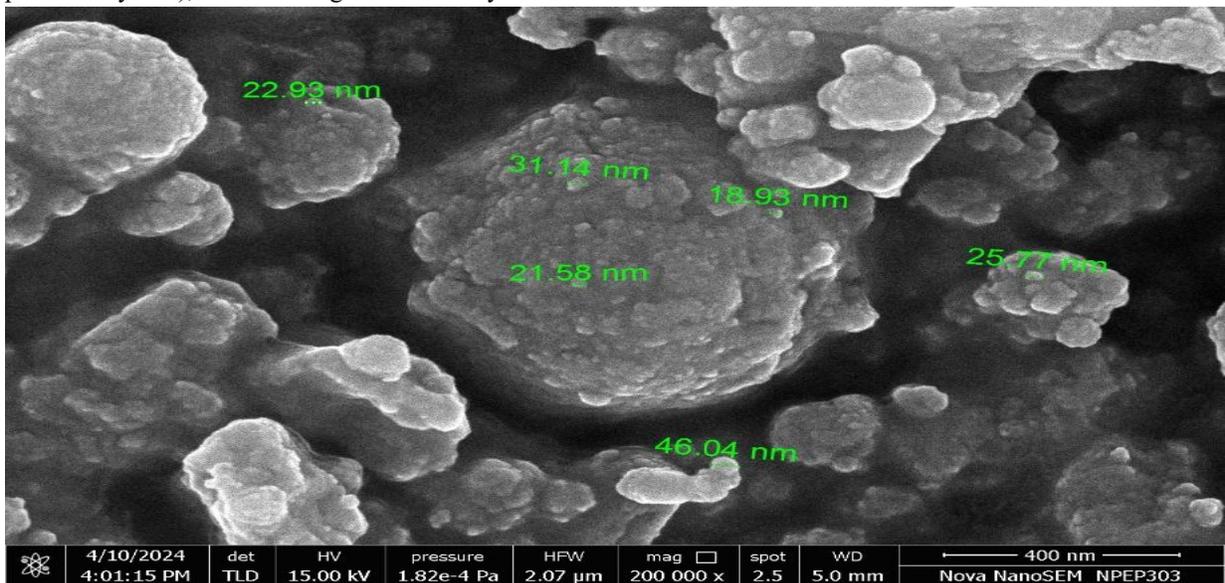

Fig 3: Surface Morphology of $BiFeO_3$

The nanoparticles appear to have irregular shapes with rough surfaces, which may enhance surface area. This characteristic can be advantageous for catalytic and adsorption-based applications. There is evident agglomeration, where smaller nanoparticles cluster to form larger assemblies. The particles exhibit a mix of spherical and irregularly shaped structures.

3.3. Energy Dispersive X-ray Spectroscopy (EDS) Analysis of $BiFeO_3$:

The energy-dispersive X-ray spectroscopy was used to evaluate the chemical composition of bismuth ferrite nanoparticles. This analysis clearly showed the identification strong peaks of bismuth ferrite (Bi) and ferrite (Fe) elements.
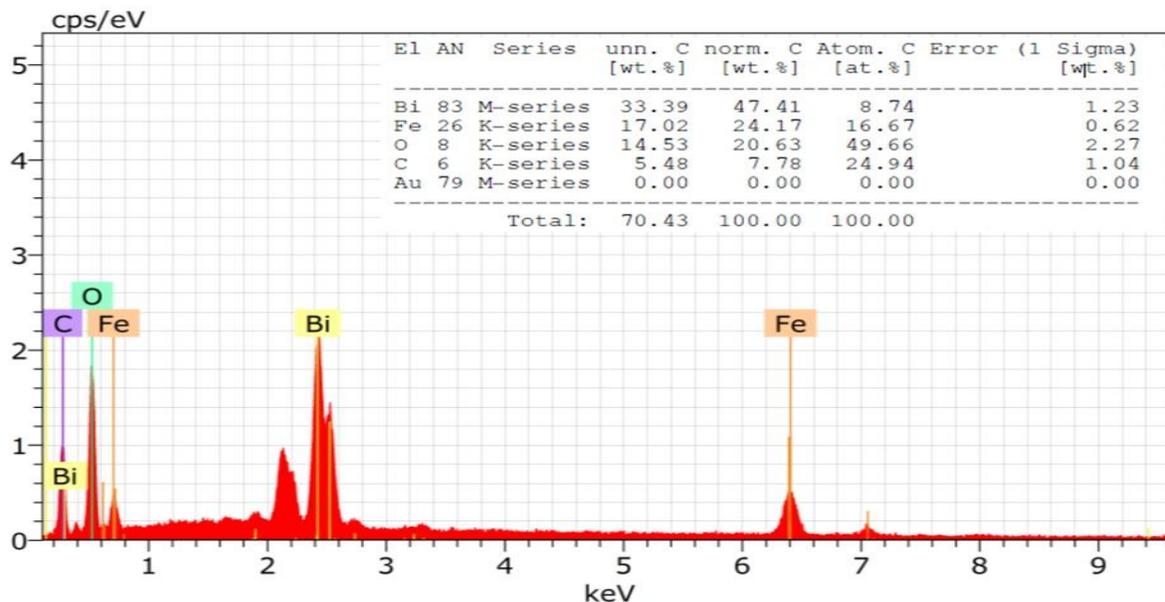

El	AN	Series	unn. C [wt.%]	norm. C [wt.%]	Atom. C [at.%]	Error (1 Sigma) [wt.%]
Bi	83	M-series	33.39	47.41	8.74	1.23
Fe	26	K-series	17.02	24.17	16.67	0.62
O	8	K-series	14.53	20.63	49.66	2.27
C	6	K-series	5.48	7.78	24.94	1.04
Au	79	M-series	0.00	0.00	0.00	0.00
		Total:	70.43	100.00	100.00	

Fig:4 The energy dispersive spectroscopy (EDS) of $BiFeO_3$

The Energy Dispersive X-ray Spectroscopy (EDS) spectrum of the synthesized $BiFeO_3$ sample confirms the elemental composition and purity of the material. The detected elements and their corresponding weight percentages (wt.%) are listed in the table within the spectrum. The primary elements identified include bismuth (Bi), iron (Fe), and oxygen (O), which are the essential constituents of $BiFeO_3$. Additionally, carbon (C) is present in small amounts, likely due to sample preparation or contamination, while gold (Au) appears with negligible content, possibly from the conductive coating applied for EDS analysis.

The dominant peaks correspond to the Bi M-series, Fe K-series, and O K-series, which are consistent with the expected elemental composition of $BiFeO_3$. The Bi M-series peak around 2.4 keV is prominent, confirming the presence of bismuth ferrite. The Fe K-series peak at approximately 6.4 keV is also well-defined, indicating significant iron content. The O K-series peak around 0.5 keV suggests the presence of oxygen, which plays a crucial role in the perovskite structure.

Quantitative analysis shows that bismuth constitutes approximately 47.41 wt.%, iron 24.17 wt.%, and oxygen 20.63 wt.%, which aligns with the expected stoichiometric composition of $BiFeO_3$. The atomic percentage (at. %) values further support this finding, with oxygen having the highest atomic concentration (49.66 at. %), followed by iron (16.67 at. %) and bismuth (8.74 at. %). The presence of carbon (7.78 at. %) is attributed to residual organic compounds or contamination from the sample holder. The absence of significant impurities further supports the high purity of the synthesized $BiFeO_3$ material.

Overall, the EDS results confirm the successful synthesis of $BiFeO_3$ with a composition close to the theoretical stoichiometry. The elemental distribution and peak intensities indicate the formation of a uniform phase, making the sample suitable for further structural and functional property investigations.

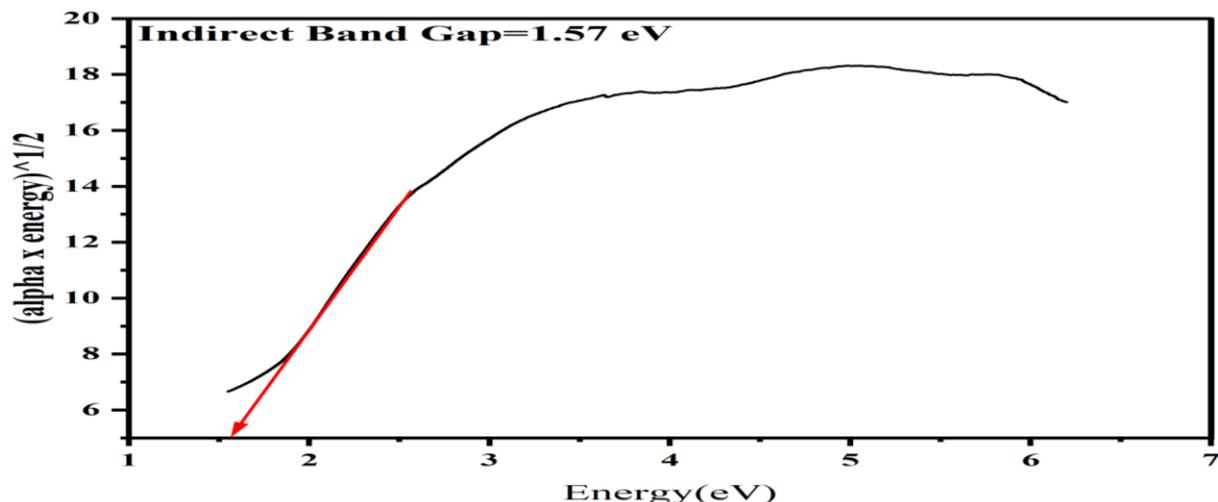### 3.4. Electronic Absorption spectra:

Fig.5 Electronic Absorption spectra of BiFeO₃

The optical band gap of the synthesized $BiFeO_3$ sample was determined using the Tauc plot, as shown in the Fig. 5. The plot represents the relationship between photon energy (hν) and the absorption coefficient (α) raised to the power of 1/2, which is characteristic of an indirect band gap semiconductor. The extrapolation of the linear region of the $(\alpha h\nu)^{1/2}$ vs. hν curve to the energy axis yields an indirect band gap energy of approximately 1.57 eV. The obtained band gap value is consistent with previously reported values for $BiFeO_3$, which typically range between 1.5 and 2.7 eV [19], depending on factors such as synthesis conditions, grain size, and structural defects. The relatively low band gap of 1.57 eV suggests that the synthesized $BiFeO_3$ sample has strong absorption in the visible region, making it a promising material for photocatalytic activity. Additionally, the presence of structural defects or oxygen vacancies could contribute to a slight reduction in the band gap, which may enhance its photocatalytic activity under visible light irradiation.

3.5. Fourier Transform Infrared Spectroscopy (FTIR) Analysis:

The Fourier Transform Infrared Spectroscopy (FTIR) spectrum of the synthesized $BiFeO_3$ sample, shown in the Fig. 6, provides insights into the vibrational modes of the material and confirms the presence of functional groups associated with the perovskite structure. The spectrum was recorded in the range of 4000–500 cm⁻¹, with several characteristic absorption bands observed at different wavenumbers.

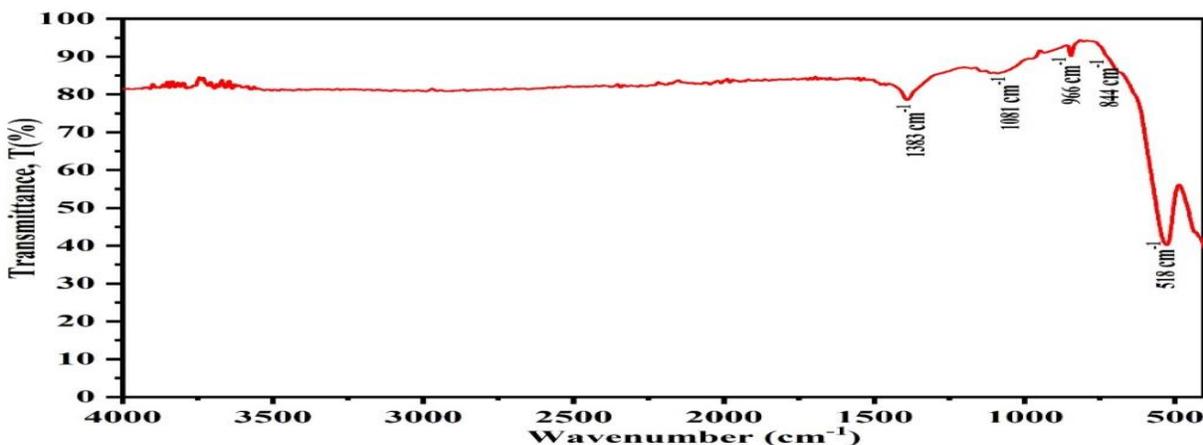The table 1 provides a clear and concise summary of the FTIR peak analysis for $BiFeO_3$.

Fig.6: FTIR analysis of BiFeO₃ at 500°C

Table 1: FTIR analysis of BiFeO₃ at 500°C

Wavenumber (cm^{-1})	Assignment	Description	Ref.
518 cm^{-1}	Fe–O stretching	Characteristic peak for the perovskite BiFeO$_3$ phase.	[20]
844 cm^{-1}	Bi–O vibrations	Confirms the formation of BiFeO$_3$	[21]
906 cm^{-1}	Fe–O–Fe / Bi–O vibrations	Indicates structural distortions in the BiFeO$_3$ lattice.	[22]
1081 cm^{-1}	C–O stretching	Suggests minor organic or carbonate impurities.	[22]
1383 cm^{-1}	NO$_3^-$ bending	May be due to residual nitrates from precursor materials.	[22]
3000–3500 cm^{-1}	Hydroxyl (-OH) group	Absence of peaks suggests minimal moisture or hydroxyl contamination.	[22]

IV. CONCLUSION

In the present study, the BiFeO$_3$ nanoparticles were prepared by green synthesis method by using *Neuracanthus trinervius* ethanolic extract. The XRD spectrum confirmed that the sample predominantly belongs to the rhombohedral perovskite crystallite structure and the crystallite size calculated by Scherrer formula is approximately 16.52 nm. The SEM images show particle size between the 18.93 nm to 46.04 nm of BiFeO$_3$. The EDS results confirm, the elemental distribution and peak intensities indicate the formation of a uniform phase, making the sample suitable for further structural and functional property investigations. The Tauc plot analysis confirms the semiconductor nature of BiFeO$_3$ has indirect band 1.5 eV and highlights its potential for applications that require efficient light absorption in the visible range. The FTIR spectrum confirms the successful formation of BiFeO$_3$ with characteristic Fe–O vibrational modes. The absence of hydroxyl peaks indicates good phase purity and stability of the synthesized material.

REFERENCES

[1] Chaudhry N, Dwivedi S, Chaudhry V, Singh A, Saquib Q, Azam A, et al. Bioinspired nanomaterials in agriculture and food: Current status, foreseen applications and challenges. Microbial Pathogenesis. 2018;123:196-200. DOI: 10.1016/j.micpath.2018.07.013

[2] Kolahalam LA, Kasi Viswanath IV, Diwakar BS, Govindh B, Reddy V, Murthy YLN. Review on nanomaterials: Synthesis and applications. Materials Today: Proceedings. 2019;18:2182-2190. DOI: 10.1016/j.matpr.2019.07.371

[3] Iravani S, Korbekandi H, Mirmohammadi SV, Zolfaghari B. Synthesis of silver nanoparticles: Chemical, physical and biological methods. Research in Pharmaceutical Sciences. 2014;9(6):385-406

[4] Mustapha T, Misni N, Ithnin NR, Daskum AM, Unyah NZ. A review on plants and microorganisms mediated synthesis of silver nanoparticles, role of plants metabolites and applications. International Journal of Environmental Research and Public Health. 2022;19(2):674. DOI: 10.3390/ ijerph19020674

[5] Fan HT, Pan SS, Teng XM, Ye C, Li GH, and Zhang LD. δ-Bi2O3 thin films prepared by reactive sputtering: Fabrication and characterization. Thin Solid Films (2006) 513: 142-7.

[6] Mharsale, N. N., More, P. S., Khollam, Y. B., Shaikh, S. F., Al-Enizi, A. M., & Gadakh, S. R. (2024). Visible light-induced photocatalytic degradation of methylene blue dye using pure phase bismuth ferrite nanoparticles. *Journal of Physics and Chemistry of Solids*, *192*, 112049.

[7] Gao, T., Chen, Z., Zhu, Y., Niu, F., Huang, Q., Qin, L., ... & Huang, Y. (2014). Synthesis of BiFeO3 nanoparticles for the visible-light induced photocatalytic property. *Materials Research Bulletin*, *59*, 6-12. https://doi.org/10.1016/j.materresbull.2014.06.022

[8] Gao, J., Wei, Z., Yuan, M., Wang, Z., Lü, Z., Li, Q., ... & Wei, B. (2024). Boosting oxygen

reduction activity and CO2 resistance on bismuth ferrite-based perovskite cathode for low-temperature solid oxide fuel cells below 600° C. Journal of Energy Chemistry, 90, 600-609.

[9] Maricar, S. M. M. S., Sastikumar, D., Vanga, P. R., & Ashok, M. (2021). BiFeO3 clad modified fiber optic gas sensor for room temperature applications. Materials Today: Proceedings, 39, 245-249.

[10] Rusevova, K., Köferstein, R., Rosell, M., Richnow, H. H., Kopinke, F. D., & Georgi, A. (2014). LaFeO3 and BiFeO3 perovskites as nanocatalysts for contaminant degradation in heterogeneous Fenton-like reactions. *Chemical Engineering Journal*, *239*, 322-331.

[11] Gulati, S., Goyal, K., Arora, A., Kumar, S., Trivedi, M., & Jain, S. (2022). Bismuth ferrite (BiFeO 3) perovskite-based advanced nanomaterials with state-of-the-art photocatalytic performance in water clean-up. Environmental Science: Water Research & Technology, 8(8), 1590-1618.

[12] Yang, S. Y., Martin, L. W., Byrnes, S. J., Conry, T. E., Basu, S. R., Paran, D., ... & Ramesh, R. (2009). Photovoltaic effects in BiFeO3. Applied Physics Letters, 95(6).

[13] Pattanayak, D., Pattanayak, S., & Rout, C. (2024). Oxide Phases in Bismuth Ferrite (BFO)—Key for Photovoltaic Application. In Iron Oxide-Based Nanocomposites and Nanoenzymes: Fundamentals and Applications (pp. 139-155). Cham: Springer International Publishing.

[14] Sulaiman, N. F., Abd Mubin, M. H., Gunasekaran, S. S., Sofiah, A. G. N., Chaudhary, K. T., Mohamad, S. N., & Ali, J. (2025). Optimization using RSM-CCD in the fabrication of magnesium-doped bismuth ferrite nanoparticles via sol–gel auto-combustion method for enhanced photocatalytic performance. Results in Physics, 69, 108114.

[15] Sun, Q., Wang, Z., He, H., Liu, H., Li, H., & Tang, X. (2025). Fabrication and photodynamic antimicrobial property analysis of BiFeO3 composite photocatalytic. Vacuum, 114338.

[16] Bidgood, S., & Brummitt, R. K. (1998). A revision of the genus Neuracanthus (Acanthaceae). Kew Bulletin, 1-76.

[17] Sally Bidgood and R. K. Brummitt "A Revision of the Genus *Neuracanthus* (Acanthaceae)." Kew Bulletin, Vol. 53, No. 1 (1998), pp. 1-76

[18] Mharsale, N. N., More, S. G., More, M. A., Shinde, S. D., Patil, G. E., & Gadakh, S. R. (2025). Chelating agent assisted BiFeO3 nanostructured material for visible light induced photocatalytic degradation of methylene blue dye. Journal of Sol-Gel Science and Technology, 113(2), 344-355.

[19] Benyoussef, M., Nassereddine, Y., Saitzek, S., Blach, J. F., El Marssi, M., Sayede, A., & Jouiad, M. (2025). A comparative study of BiFeO3-based compounds for enhanced hydrogen evolution reaction. Fuel, 381, 133579.

[20] Nazir, A., Latif, S., Adil, S. F., Kuniyil, M., Imran, M., Hatshan, M. R., & Shaik, B. (2021). Photocatalytic degradation of cefixime trihydrate by bismuth ferrite nanoparticles. Materials, 15(1), 213.

[21] Sarkar, K., Harsh, H., Rahman, Z., & Kumar, V. (2024). Enhancing the structural, optical, magnetic and ferroelectric properties of perovskite BiFeO3 through metal substitution. Chemical Physics Impact, 8, 100478.

[22] Petrukhin, D., Salnikov, V., Nikitin, A., Sidane, I., Slimani, S., Alberti, S., & Rodionova, V. (2024). Effect of Bismuth Ferrite Nanoparticles on Physicochemical Properties of Polyvinylidene Fluoride-Based Nanocomposites. Journal of Composites Science, 8(8), 329.